Output Feedback Event-triggered Control of Doubly Fed Induction Generators For Wind Turbines

Mahmoud Abdelrahim
Dep. of Communications and Networks Eng.
Prince Sultan University
Riyadh, Saudi Arabia
Dep. of Mechatronics Eng.
Assiut University
Assiut, Egypt
mabdelrahim@psu.edu.sa
m.abdelrahim@aun.edu.eg

Michele Cucuzzella
Dep. of Elec., Computer and Biomedical Eng.
University of Pavia
Pavia, Italy
michele.cucuzzella@unipv.it

Dhafer Almakhles
Dep. of Communications and Networks Eng.
Prince Sultan University
Riyadh, Saudi Arabia
dalmakhles@psu.edu.sa

***Abstract*— We consider the problem of pitch angle control for doubly fed induction generators in wind turbines affected by external disturbances. We assume that only an output measurement is available and the feedback signal is transmitted over a digital channel to the controller. An event-triggered control algorithm is developed to produce the transmission instants of the output measurement. We follow the emulation approach in the sense that we first stabilize the plant in continuous-time where we synthesize a robust control methodology based on the Linear Quadratic Gaussian Regulator (LQG) approach. Then, we consider the effect of the network and we construct an event-triggering mechanism such that the closed-loop stability is preserved while the Zeno phenomenon is prevented by means of time regularization. The overall system is modelled as a hybrid dynamical system and the required stability conditions are formulated in terms of a linear matrix inequality. The effectiveness of the control method is illustrated by simulation on a numerical model of the DFIG wind turbine.**

I. Introduction

The integration of renewable energy resources (RES) such as photovoltaic, wind and geothermal energy with traditional electric grids has received a great attention in the last decades due to the increased power demand and the scarcity of fossil fuels as well as the issues related to climate change. Among the RES, wind farms have a huge potential to provide energy to the grid by means of wind turbines (WTs), which can be classified to either fixed speed or variable speed WTs. In the fixed speed type, the WT generator is directly connected to the grid while in the variable speed framework, the generator is controlled by some power electronic converters. A commonly used type of AC generators for variable speed wind turbines is the induction generator, in particular, doubly fed induction generators (DFIG). In DFIG, the stator winding is directly connected to grid while the rotor winding is connected to the grid via two back-to-back converters: a rotor side and a grid side converter. The DFIG has several advantages compared to other types of induction generators in terms of robustness and stable operation against external disturbances.

* This work was supported by the Prince Sultan University.

The main task of wind turbine controllers is to provide appropriate integration of the wind farm with the local grid in terms of supply-demand matching. Such power balance is often achieved by controlling the rotational speed of the wind turbine generator. Several control schemes have been proposed in the literature for DFIG-based wind turbines in continuous-time, e.g. [1]–[6] and discrete-time, e.g. [7]–[10]. However, in practice it is often the case that the plant output is measured by analog sensors while the controller is a digital platform. Moreover, in some cases the plant and the controller cannot be co-located and hence they need to communicate over a shared digital channel, i.e., networked control systems, which produces network-induced errors and makes more challenging the control design [11]–[13]. Specifically, one of the issues due to the digital implementation is sampling effect, which can lead to a serious degradation of the system performance or even to instability. Traditionally, the sampling effect is treated using time-triggering approaches, where the stabilizing sampling frequency is determined based on the worst case scenario, which can be conservative to implement in practice. Alternatively, the event-triggered control has been developed in the literature, where the sampling instants are computed based on a state dependent rule according to the desired stability properties and the current system state. In this way, the amount of transmissions can be greatly reduced compared to periodic sampling, see, e.g. [14]–[19] and the references therein. In order to be implementable in practice, the triggering conditions have to prevent the occurrence of Zeno behaviour, i.e., infinite transmissions in a finite time. This issue becomes more challenging when only the output of the plant can be measured and the plant is affected by external disturbances.

To the best of our knowledge, the problem of event-triggered control (ETC) of DFIG-based wind turbines has been studied in a few works in the literature [20]–[22]. The ETC mechanisms proposed in [20], [21] rely on the availability of full state measurements, which might not be feasible in practice. Compared to those results, in this paper, we study the case where the wind turbine is affected by external disturbances such as wind speed variations and

change in power demand while only the shaft speed of the wind turbine is available for measurement. Moreover, the event-triggering mechanism, the stabilizing control technique and the derived robustness property are different from those developed in the previously mentioned results. In addition, we model the overall system as a hybrid dynamical systems to provide a more accurate model to such networked control system, which has not been done in [20], [22].

We consider the problem of robust stabilization of a DFIG-based wind turbine by using LQG feedback law. We assume that only the angular speed of the wind turbine shaft can be measured and transmitted to the controller over a digital channel at discrete-time instants. Then, we synthesize an output feedback event-triggering mechanism such that the closed-loop stability is maintained, while the Zeno behaviour is avoided. The latter property is achieved by enforcing a strictly positive lower bound on the inter-transmission intervals, which is known as time regularization. The closed-loop system exhibits both continuous-time dynamics and discrete transitions due to the sampling errors induced by the network. To cope with such combined dynamics, we formulate the overall system as a hybrid dynamical system using the formalism in [23]. The required conditions are formulated in a systemic way in terms of the feasibility of a linear matrix inequality (LMI). The developed approach ensures an $\mathcal{L}_2$-stability for the closed-loop system. The effectiveness of the approach is demonstrated by numerical simulation. The results reveal an interesting trade-off between the obtained $\mathcal{L}_2$-gain and the amount of transmissions, which is beneficial in practice.

The contribution of this paper can be summarized below

- a robust output feedback event-triggered controller for a DFIG-based wind turbine is developed;
- the closoed-loop system is modeled as a hybrid dynamical system to capture the sampled-data nature of the control system;
- a trade-off between the ensured stability property and the generated amount of transmissions is revealed.

The remainder of this paper is organized as follows. Preliminaries are given in Section II and the problem is formulated in Section III. The hybrid dynamical model of the closed-loop system is presented in Section IV. Then, we synthesize the proposed feedback law and the event-triggering mechanism in Section V and we state the obtained stability result in Section VI. The simulation is presented in Section VII. The conclusions are given in Section VIII.

II. Preliminaries

Let $\mathbb{R} := (-\infty, \infty)$, $\mathbb{R}_{\geq 0} := [0, \infty)$, $\mathbb{N} := \{0, 1, 2, \ldots\}$ and $\mathbb{N}_{>0} := \{1, 2, \ldots\}$. We denote the minimum and maximum eigenvalues of the real symmetric matrix A as $\lambda_{\min}(A)$ and $\lambda_{\max}(A)$, respectively. We write A^T to denote the transpose of A, and $\mathbb{I}_n$ stands for the identity matrix of dimension n. The symbol $\star$ stands for symmetric blocks. We write $(x, y) \in \mathbb{R}^{n_x+n_y}$ to represent the vector $[x^T, y^T]^T$ for $x \in \mathbb{R}^{n_x}$ and $y \in \mathbb{R}^{n_y}$. For a vector $x \in \mathbb{R}^{n_x}$, we denote by $|x| := \sqrt{x^T x}$ its Euclidean norm and, for a matrix $A \in \mathbb{R}^{n\times m}$, $|A| := \sqrt{\lambda_{\max}(A^T A)}$.

We consider hybrid systems of the following form [23]

$$\dot{x} = F(x) \quad x \in \mathcal{C}, \qquad x^+ \in G(x) \quad x \in \mathcal{D}, \tag{1}$$

where $x \in \mathbb{R}^{n_x}$ is the state, $\mathcal{C}$ is the flow set, F is the flow map, $\mathcal{D}$ is the jump set and G is the jump map. Solutions to system (1) are defined on *hybrid time domains*.

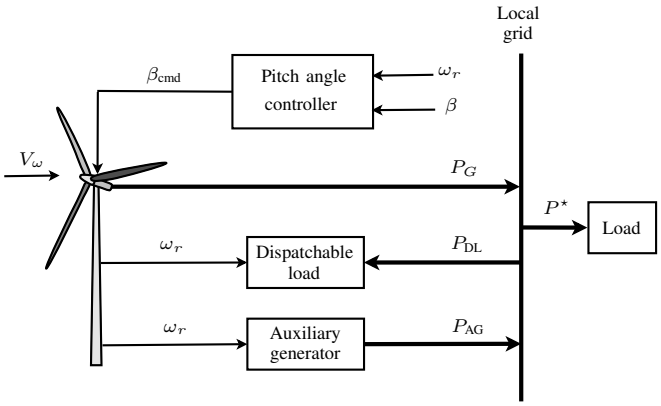

Fig. 1. Layout of DFIG-based wind turbine control.

III. Problem Formulation

The local grid that we consider mainly consists of four components: a wind turbine, a load, an auxiliary generator and a dispatchable load, see Figure 1. We assume that the load power demand $P^\star$ is fully provided by the power P_G extracted from the wind turbine. The task of the controller is to adjust the output power according to the change of power demand by regulating the pitch angle of the wind turbine. When the power $P^\star$ required by the load exceeds the extracted power from the wind turbine, an external power P_{AG} is provided by an auxiliary generator such as a diesel generator. On the other hand, when $P_G > P^\star$, i.e., if the power generated by the wind turbine is greater than the power demand and the pitch control action is not fast enough, a dispatchable load such as resistors bank or irrigation system is employed to dissipate the excess power P_{DL}. The auxiliary generator and the dispatchable load are orchestrated by means of an energy management system (EMS) [24].

The linearized model of the considered system is given by [24]

$$\begin{aligned}\dot{\beta}(t) &= \frac{-1}{\tau_\beta}\beta(t) + \frac{-1}{\tau_\beta}\beta_{\text{cmd}}(t)\\ \dot{\omega}_r(t) &= \frac{M_3}{J}\beta(t) + (\frac{M_2}{J} + \frac{P^\star}{J\omega_0^2})\omega_r(t) + \frac{-1}{J\omega_0}\delta_{P^\star}(t)\\ &\quad + \frac{M_1}{J}\delta_{V_w}(t),\end{aligned} \tag{2}$$

where $\beta(t)$, $\omega_r(t)$ are the pitch angle and the shaft angular speed of the wind turbine, respectively, $\beta_{\text{cmd}}(t)$ is the command signal from the controller to adjust the pitch angle, $\delta_{P^\star}(t)$ and $\delta_{V_w}(t)$ are the variations in power demand and

wind speed, respectively. The parameters τ_β, J denote the time constant of the wind turbine blade and the moment of inertia, respectively, $P^\star$ is the load power demand and the parameters $J\omega_0$ refer to the moment of inertia J at the angular speed linearization ω_0. The coefficients M_1, M_2, M_3 are functions of the constant parameters of the wind turbine and their expressions can be found in [24]. We assume that only the angular speed ω_r can be measured. Hence, the state space model of DFIG is given by

$$\begin{aligned} \dot{x}_p(t) &= Ax_p(t) + Bu(t) + Ew(t) \\ y(t) &= Cx_p(t), \end{aligned} \tag{3}$$

where $x_p(t) := (\beta(t), \omega_r(t))$ is the state vector, $u(t) := \beta_{\text{cmd}}(t)$ is the control signal, $w(t) := (\delta_{P^\star}(t), \delta_{V_w}(t))$ gathers the external disturbances and y is the measured output. The dimensions of x_p, u, d, y are $x_p \in \mathbb{R}^{n_p}$, $u \in \mathbb{R}^{n_u}$, $w \in \mathbb{R}^{n_d}$ and $y \in \mathbb{R}^{n_y}$. The matrices A, B, C, E are give by

$$\begin{aligned} A &= \begin{bmatrix} \dfrac{-1}{\tau_\beta} & 0 \\ \dfrac{M_3}{J} & \left(\dfrac{M_2}{J} + \dfrac{P^\star}{J\omega_0^2}\right) \end{bmatrix}, \quad B = \begin{bmatrix} \dfrac{1}{\tau_\beta} \\ 0 \end{bmatrix} \\ E &= \begin{bmatrix} 0 & 0 \\ \dfrac{-1}{J\omega_0} & \dfrac{M_1}{J} \end{bmatrix}, \quad C = \begin{bmatrix} 0 & 1 \end{bmatrix}. \end{aligned} \tag{4}$$

Since only the output y is available for measurement rather than the full state x, we stabilize the system by an observer-based controller of the following form

$$\begin{aligned} \dot{x}_c(t) &= Ax_c(t) + Bu(t) + L(y(t) - Cx_c(t)) \\ u(t) &= -Kx_c(t), \end{aligned} \tag{5}$$

where $x_c \in \mathbb{R}^{n_c}$ denotes the estimated state and L, K are the observer and the controller gain matrices, respectively. The controllability and the observability matrices, respectively denoted by M_c and M_o, are given by

$$M_c = [B \quad AB] = \begin{bmatrix} \dfrac{1}{\tau_\beta} & \dfrac{-1}{\tau_\beta^2} \\ 0 & \dfrac{M_3}{J\tau_\beta} \end{bmatrix} \tag{6}$$

and

$$M_o = \begin{bmatrix} C \\ CA \end{bmatrix} = \begin{bmatrix} 0 & 1 \\ \dfrac{M_3}{J} & \left(\dfrac{M_2}{J} + \dfrac{P^\star}{J\omega_0^2}\right) \end{bmatrix}. \tag{7}$$

It is clear that both the controllability and the observability matrices have full rank, i.e., the pair (A, B) is controllable and the pair (A, C) is observable, for any values of the DFIG system parameters. Consequently, the controller and the observer gains K and L can be always found to make the closed-loop matrices $A - BK$ and $A - LC$ are Hurwitz.

We now take into account the effect of the communication network since the output measurement y is assumed to be transmitted over a digital channel while the controller is directly fed to the plant. Consequently, the control input u is updated only at discrete time instants $t_k, k \in N$. In order to reduce the amount of transmissions, we consider the scenario where the sequence of transmission instants $t_k, k \in N$ is produced by an output feedback event-triggering condition that will be designed in the next section. Between two transmission instants, the transmitted output measurement $y(t_k)$ is kept constant by a Zero-Order-Hold (ZOH). As a result, in view of (3)–(5), the closed-loop system can be described by

$$\left.\begin{aligned} \dot{x}_p(t) &= Ax_p(t) - BKx_c(t) + Ew(t) \\ u(t) &= -Kx_c(t) \\ y(t) &= Cx_p(t) \end{aligned}\right\} \quad \forall t \in \mathbb{R}$$

$$\left.\begin{aligned} \dot{x}_c(t) &= (A - BK - LC)x_c(t) + Ly(t_k) \\ \dot{y}(t_k) &= 0 \end{aligned}\right\} \quad \forall t \in [t_k, t_{k+1}). \tag{8}$$

IV. Hybrid Dynamical Model

We present the hybrid dynamical model of the closed-loop system. Define the sampling induced error of the output measurement as follows

$$e(t) = y(t_k) - y(t) \qquad \forall t \in [t_k, t_{k+1}). \tag{9}$$

Note that at each transmission instant, the last transmitted value $y(t_k)$ is updated to the actual value $y(t)$, i.e., the sampling error $e(t)$ is reset to zero at each transmission instant. Hence, we have

$$\begin{aligned} \dot{e}(t) &= -\dot{y}(t) = -CAx_p(t) + CBKx_c(t) - CEw(t) \\ y(t_k^+) &= y(t_k) \\ e(t_k^+) &= 0. \end{aligned} \tag{10}$$

By substituting (9) in (8), we obtain

$$\begin{aligned} \dot{x}_p(t) &= Ax_p(t) - BKx_c(t) + Ew(t) \\ \dot{x}_c(t) &= (A - BK - LC)x_c(t) + Ly(t) + Le(t) \end{aligned} \tag{11}$$

Define $x := (x_p, x_c) \in \mathbb{R}^{n_x}$ with $n_x := n_p + n_c$, then

$$\begin{aligned} \dot{x}(t) &= \begin{bmatrix} A & -BK \\ LC & (A - BK - LC) \end{bmatrix} x(t) + \begin{bmatrix} 0 \\ L \end{bmatrix} e(t) + \begin{bmatrix} E \\ 0 \end{bmatrix} w(t) \\ &=: \mathcal{A}_1 x(t) + \mathcal{B}_1 e(t) + \mathcal{E}_1 w(t). \end{aligned} \tag{12}$$

It is evident that the sampled-data system is naturally a hybrid dynamical system due to the iterations between continuous-time and discrete-time dynamics. We use the framework of [23] to model the overall system in which the *flow dynamics* refers to the continuous-time behaviour and the *jump dynamics* refers to the discrete-time changes of the closed-loop system. Moreover, the conditions at which the system is running in continuous- or discrete-time are denoted

by the *flow set* and the *jump set*, respectively, we refer the reader to [23] for more details.

To this end, we need to introduce an auxiliary time variable with the following dynamics

$$\dot{\tau}(t) = 1 \quad \forall t \in [t_k, t_{k+1}), \qquad \tau(t_k^+) = 0. \tag{13}$$

Let $\xi := (x, e, \tau) \in \mathbb{R}^{n_x} \times \mathbb{R}^{n_y} \times \mathbb{R}$. Then, the hybrid dynamical system is given by

$$\begin{aligned} \dot{\xi}(t) &\in \begin{bmatrix} \mathcal{A}_1 x(t) + \mathcal{B}_1 e(t) + \mathcal{E}_1 w(t) \\ \mathcal{A}_2 x(t) + \mathcal{E}_2 w(t) \\ 1 \end{bmatrix}, \quad && \xi(t) \in \mathcal{C} \\ \xi(t_k^+) &\in \begin{bmatrix} x \\ 0 \\ 0 \end{bmatrix}, && \xi(t) \in \mathcal{D}, \end{aligned} \tag{14}$$

where $\mathcal{A}_2 := [-CA \;\; CBK]$ and $\mathcal{E}_2 := -CE$. The flow and jump sets $\mathcal{C}, \mathcal{D}$ are defined based on the event-triggering rule as will be developed in the next section.

V. Event-Triggered Control Design

We design the event-triggered controller by following the emulation approach in the sense that we first stabilize the plant without considering the communication network and then we take into account the sampling induced error. Then, we derive an event-triggering rule that maintains the closed-loop stability.

A. LQG Feedback Law

First, let us assume that the full state measurement is available, i.e., $y = x$. Then, we can design an LQR controller to strike a balance between the state response and the control effort by using the following quadratic cost function

$$J = \int_0^\infty (x^T Q_1 x + u^T R_1 u) dt, \tag{15}$$

where Q_1, R_1 are symmetric positive definite diagonal matrices. Then, by solving the algebraic Riccati equation

$$A^T P_1 + P_1 A + Q_1 - P_1 B R_1^{-1} B^T P_1 = 0 \tag{16}$$

the optimal state feedback law is given by $u = -K x_p$ with

$$K = R_1^{-1} B^T P_1. \tag{17}$$

Now we consider that only an output y is measured but not the full state. Then, we employ the state observer in (5) to estimate the state. Since the wind turbine is affected by external disturbance, we apply the Kalman filter to deign the observer gain L by solving the following algebraic Riccati equation

$$P_2 A^T + A P_2 + Q_2 - P_1 C^T R_2^{-1} C P_2 = 0, \tag{18}$$

where Q_2, R_2 are symmetric positive definite diagonal matrices. Consequently, the observer gain (Kalman gain) L is given by

$$L = P_2 C^T R_2^{-1}. \tag{19}$$

Note that the design of Kalman filter is a dual task to the LQR design. Moreover, the gain matrices K and L can be designed separately by following the superposition principle of linear systems. We note that the existence of solutions to the algebraic Riccati equations (16) and (18) is guaranteed since the closed-loop system is both controllable and observable as explained in (6) and (7).

B. Event-triggering Rule

We now consider the effect of the communication network and we construct an output feedback event-triggering condition such that the closed-loop stability is maintained. One of the main issues to handle in the design of ETC is to prevent the occurrence of the Zeno behavior, which is particularly challenging when only the output y is measured and the plant is affected by external disturbances. An effective approach to overcome this issue is by enforcing a strictly positive minimum time T on the inter-transmission intervals by using the time-regularization technique, see e.g. [25], [26], [27]. In this way, the ETC condition takes the following form

$$t_{k+1} = \inf\{t \geq t_k + T : \;\; |e(t)| \geq \sigma |y(t)|\}, \tag{20}$$

where $\sigma, T > 0$ are design parameters to be specified later. Condition (20) implies that a new transmission instant t_{k+1} is allowed only after the elapse of time T since the last triggering instant t_k and such that $|e(t)| \geq \sigma |y(t)|$ is satisfied. As a consequence, the flow and jump sets in (14) are given by

$$\begin{aligned} \mathcal{C} &= \big\{\xi(t) : |e(t)| \leq \sigma |y(t)| \;\text{ or }\; \tau \in [0, T]\big\} \\ \mathcal{D} &= \big\{\xi(t) : |e(t)| \geq \sigma |y(t)| \;\text{ and }\; \tau \geq T\big\}. \end{aligned} \tag{21}$$

The enforced minimum time T is designed based on the so-called *Maximally Allowable Transmission Interval (MATI)* bound developed in [28], [29] such that T is upper bounded by the MATI. Hence, similar to [29], [30], we need to impose the following conditions on the hybrid dynamical system (14) to ensure the closed-loop stability.

Assumption 1: Consider the hybrid system (14), (21). There exist $\varepsilon, \gamma, \eta > 0$ and a positive definite symmetric real matrix P such that the following condition holds.

$$\begin{bmatrix} \mathcal{A}_1^T \boldsymbol{P} + \boldsymbol{P} \mathcal{A}_1 + (1+\varepsilon) C^T C & \star & \star \\ \mathcal{B}_1^T \boldsymbol{P} & -\gamma^2 \mathbb{I}_{n_y} & \star \\ \mathcal{E}_1^T \boldsymbol{P} + \mathcal{E}_2^T \mathcal{A}_2 & 0 & \mathcal{E}_2^T \mathcal{E}_2 - \boldsymbol{\eta} \mathbb{I}_{n_w} \end{bmatrix} < 0. \tag{22}$$

□

Note that, from a numerical analysis it appears that Assumption 1 is satisfied for a large range of the system parameters.

Condition (22) imposes an $\mathcal{L}_2-$gain stability from (e, w) to x with an $\mathcal{L}_2-$gain equal to $\sqrt{\eta}$. In other words, by defining $W(e) := |e|$ and $V(x) := x^T P x$, then it holds that

$$\langle \nabla W(e), \mathcal{A}_2 x(t) + \mathcal{B}_2 e(t) + \mathcal{E}_2 w(t) \rangle \quad \leq \quad H(x, w) + \beta |e|, \tag{23}$$

where $H(x,w) := |\mathcal{A}_2 x + \mathcal{E}_2 w|$ and $\beta := |\mathcal{B}_2|$. Consequently, by post- and pre-multiplying (22) by (x, e, w) and its transpose, the feasibility of (22) implies that

$$\begin{aligned}\langle \nabla V(x), \mathcal{A}_1 x(t) + \mathcal{B}_1 e(t) + \mathcal{E}_1 w(t) \rangle \leq -(1+\varepsilon)|y|^2 \\ -H^2(x,w) + \gamma^2 W^2(e) + \eta |w|^2.\end{aligned} \tag{24}$$

Note that condition (22) corresponds to Assumption 1 in [29] for nonlinear systems, which we adapt here for the LTI systems. Then, according to [29], the MATI bound is given by

$$\mathcal{T}(\gamma,\beta) := \begin{cases} \frac{1}{\beta r}\arctan(r) & \gamma > \beta \\ \frac{1}{\beta} & \gamma = \beta \\ \frac{1}{\beta r}\operatorname{arctanh}(r) & \gamma < \beta \end{cases} \tag{25}$$

with $r := \sqrt{\left|(\frac{\gamma}{\beta})^2 - 1\right|}$ and γ, β from Assumption 1.

We note that, in view of (27), if we enforce

$$\gamma^2 W^2(e) \leq \varepsilon |y|^2 \tag{26}$$

then it holds that

$$\langle \nabla V(x), \mathcal{A}_1 x(t) + \mathcal{B}_1 e(t) + \mathcal{E}_1 w(t) \rangle \leq -|y|^2 + \eta |w|^2 \tag{27}$$

which ensures that the closed-loop system is $\mathcal{L}_2$ stable. Hence, the flow and jump sets in (21) are defined with $\sigma = \frac{\sqrt{\varepsilon}}{\gamma}$ and $T \in (0, \mathcal{T}(\gamma, L))$.

VI. Stability Analysis

We are ready to state the stability result.

Theorem 1: Consider the hybrid system (14), (21) and suppose that Assumption 1 holds. Take $\sigma = \frac{\sqrt{\varepsilon}}{\gamma}$ and $T \in (0, \mathcal{T}(\gamma, L))$ in (21). Then, system (14), (21) is $\mathcal{L}_2$ stable from w to y with an $\mathcal{L}_2$-gain less than or equal to $\sqrt{\eta}$. □

The proof of Theorem 1 follows similar lines as in [30] and it is therefore omitted.

It is worth mentioning that the event-triggering mechanism (21) can be easily adapted to the case of time-triggered control by omitting the output-based rule and depending only on the elapse of the constant time T. For instance, for periodic sampling case, the flow and jump sets in (21) will be modified as follows

$$\begin{aligned}\mathcal{C} &= \{\xi(t) : \tau \in [0, T)\} \\ \mathcal{D} &= \{\xi(t) : \tau = T\}.\end{aligned} \tag{28}$$

VII. Results and Discussion

We verify the theoretical results discussed in the previous section by simulating system (3) with the parameters in Table I [24], which leads to the state space matrices

$$\begin{aligned} A &= \begin{bmatrix} -1 & 0 \\ -4.1896 & -0.0026 \end{bmatrix}, \quad B = \begin{bmatrix} 1 \\ 0 \end{bmatrix} \\ E &= \begin{bmatrix} 0 & 0 \\ 0.0137 & 22.523 \end{bmatrix}, \quad C = \begin{bmatrix} 0 & 1 \end{bmatrix}. \end{aligned} \tag{29}$$

TABLE I
Parameters of DFIG [24].

Parameter	Value
τ_β	1 s
J	180 s
P_0	5.7 kW
ω_0	300 rad/sec
M_1	4054
M_2	−0.4667
M_3	−754.123

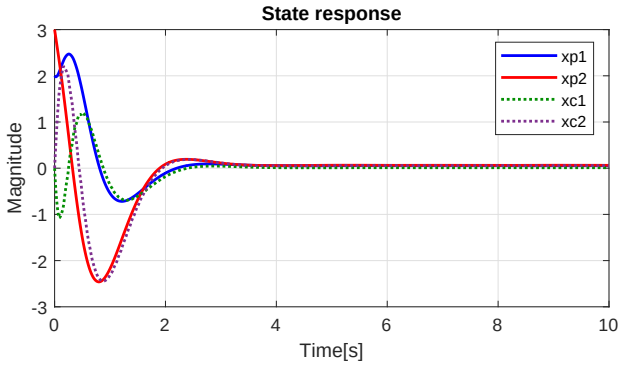

Fig. 2. Plant and observer state trajectories.

We design the controller and the observer gains as described in Section V-A with $R_1 = 0.5$ and $R_2 = 0.01$ and we obtain $K = [2.5821 \quad -1.4120]$ and $L = [-8.0408 \quad 8.2056]^T$. Then, by solving the LMI condition (22), which is feasible, we obtain the following values: $\varepsilon = 0.2013$, $\gamma = 19.6791$, $\eta = 31.6228$, which leads to $\sigma = 0.0228$, and the MATI bound $\mathcal{T}(\gamma,\beta)$ in (25) was found to be 0.0798 s. Hence, all the parameters of the ETC mechanism are determined. We run simulation with the initial condition $(x(t_0), e(t_0), \tau(t_0)) = (2, 3, 0, 0, 0, 0)$ for 10 seconds with random external disturbances satisfying $|w| < 0.5$. The minimum and the average inter-transmission intervals was found to be $\tau_{\text{min}} = T = 0.0798, \tau_{\text{avg}} = 0.1604$ seconds, respectively. Figure 2 shows that the plant and the controller states asymptotically converge to the origin. Figure 3 implies that the observer successfully estimates the plant states after a short time and then the estimation error goes to zero. Figures 4 and 5 show that the state of the closed-loop system converge to a neighbourhood of the origin due to the presence of external disturbances. The generated inter-transmission times are shown in Figure 6 and we note that the ETC mechanism significantly reduces the amount of transmissions compared to time-triggered control. Figure 7 reveals the tradeoff between the guaranteed $\mathcal{L}_2$-gain η and the triggering threshold σ (upper plot) and the enforced minimum sampling period T (lower plot). We see that when the $\mathcal{L}_2$ is enlarged, the triggering threshold σ is increased, which can lead to larger inter-transmission intervals and vice verse, see (21). Hence, this provides a tuning guide for the user according to the desired implementation properties.

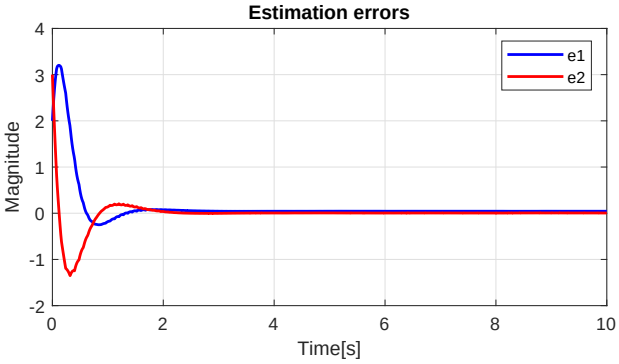

Fig. 3. Trajectories of the estimation errors.

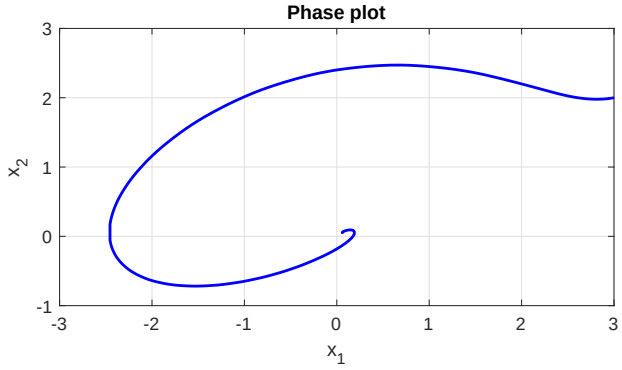

Fig. 5. Phase plot.

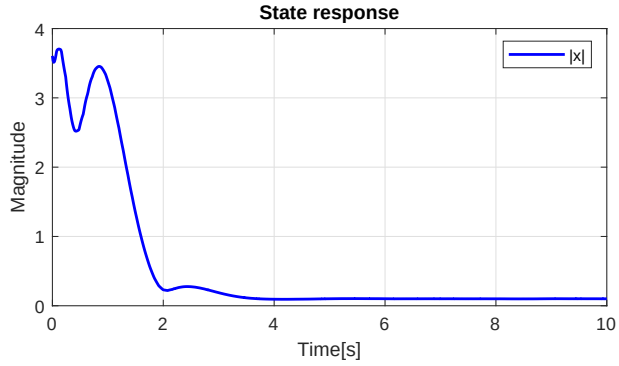

Fig. 4. Norm of state trajectories.

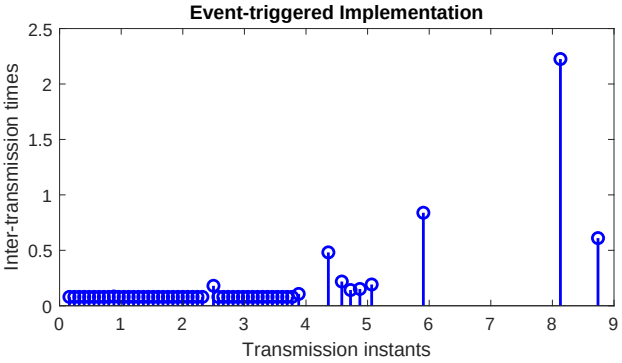

Fig. 6. Inter-transmission times.

VIII. Conclusion

Robust control design for the pitch angle of DFIG wind turbines under event-triggered implementation has been investigated. The developed approach relies only on output feedback and ensures an asymptotic stability property for the closed-loop system, preventing the occurrence of the Zeno behaviour. The overall system is modelled as a hybrid dynamical system in order to capture both continuous-time dynamics and discrete transitions. The effectiveness of the proposed approach has been illustrated numerically on a realistic model of a DFIG wind turbine. The results show that the ETC mechanism outperforms the time-triggered control by considerably reducing the amount of transmissions.

Future extension of this work may consider other digital implementation issues such as quantization, time delays and packet dropout. The investigation of periodic event-triggered control method to such systems is also relevant in practice.

References

[1] M. Nadour, A. Essadki, and T. Nasser, "Comparative analysis between PI & backstepping control strategies of DFIG driven by wind turbine," *International Journal of Renewable Energy Research*, vol. 7, pp. 1307–1316, 2017.

[2] E. Hosseini, N. Behzadfar, M. Hashemi, M. Moazzami, and M. Dehghani, "Control of pitch angle in wind turbine based on doubly fed induction generator using fuzzy logic method," *journal of renewable energy environment*, vol. 9, pp. 1–7, 2022.

[3] M. Fdaili, A. Essadki, M. Nadour, and T. Nasser, "Comparative study of MPPT and pitch angle control strategies for a wind energy conversion system," *In Proceedings of the 2017 International Renewable and Sustainable Energy Conference, Tangier, Morocco*, pp. 1–6, 2017.

[4] L. Colombo, M. Corradini, G. Ippoliti, and G. Orlando, "Pitch angle control of a wind turbine operating above the rated wind speed: A sliding mode control approach," *ISA Transactions*, vol. 96, pp. 95–102, 2020.

[5] T. Surinkaew and I. Ngamroo, "Robust power oscillation damper design for DFIG-based wind turbine based on specified structure mixed H_2/H_∞ control," *Renewable Energy*, vol. 66, pp. 15–24, 2014.

[6] G. Rigatos, P. Siano, M. Abbaszadeh, and P. Wira, "Nonlinear optimal control for wind power generators comprising a multi-mass drivetrain and a DFIG," *Journal of the Franklin Institute*, vol. 356, no. 5, pp. 2582–2605, 2019.

[7] B. Torchani, A. Sellami, and G. Garcia, "Variable speed wind turbine control by discrete-time sliding mode approach," *ISA Transactions*, vol. 62, pp. 81–86, 2016.

[8] L. Djilali, E. N. Sanchez, and M. Belkheiri, "Discrete-time neural input output feedback linearization control for a dfig based wind turbine," in *2017 6th International Conference on Systems and Control (ICSC)*, 2017, pp. 57–62.

[9] A. Tohidi, H. Hajieghrary, and M. A. Hsieh, "Adaptive disturbance rejection control scheme for dfig-based wind turbine: Theory and experiments," *IEEE Transactions on Industry Applications*, vol. 52, no. 3, pp. 2006–2015, 2016.

[10] R. Ruiz-Cruz, E. N. Sanchez, F. Ornelas-Tellez, A. G. Loukianov, and R. G. Harley, "Particle swarm optimization for discrete-time inverse optimal control of a doubly fed induction generator," *IEEE Transactions on Cybernetics*, vol. 43, no. 6, pp. 1698–1709, 2013.

[11] J. Baillieul and P. Antsaklis, "Control and communication challenges in networked real-time systems," *Proceedings of the IEEE*, vol. 95, no. 1, pp. 9–28, 2007.

[12] M. Cloosterman, L. Hetel, N. van de Wouw, W. Heemels, J. Daafouz,

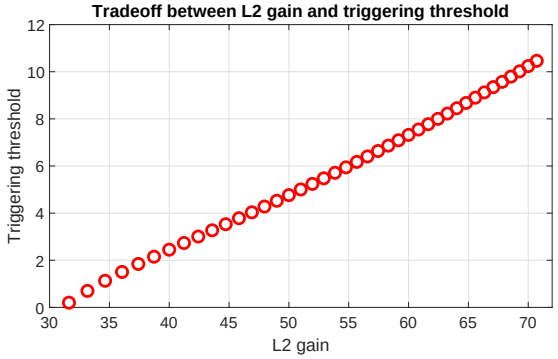

Fig. 7. Trade-off between the $\mathcal{L}_2$-gain and the parameters of ETC mechanism.

and H. Nijmeijer, "Controller synthesis for networked control systems," *Automatica*, vol. 46, no. 10, pp. 1584–1594, 2010.

[13] W. Heemels, A. Teel, N. van de Wouw, and D. Nešić, "Networked control systems with communication constraints: Tradeoffs between transmission intervals, delays and performance," *IEEE Transactions on Automatic Control*, vol. 55, no. 8, pp. 1781–1796, 2010.

[14] W. Heemels, K. Johansson, and P. Tabuada, "An introduction to event-triggered and self-triggered control," *In Proceedings of the 51st IEEE Conference on Decision and Control, Maui, U.S.A.*, pp. 3270–3285, 2012.

[15] R. Postoyan, P. Tabuada, D. Nešić, and A. Anta, "A framework for the event-triggered stabilization of nonlinear systems," *IEEE Transactions on Automatic Control*, vol. 60, no. 4, pp. 982–996, 2015.

[16] F. Forni, S. Galeani, D. Nešić, and L. Zaccarian, "Event-triggered transmission for linear control over communication channels," *Automatica*, vol. 50, no. 2, pp. 490–498, 2014.

[17] M. Abdelrahim, R. Postoyan, J. Daafouz, and D. Nešić, "Event-triggered dynamic feedback controllers for nonlinear systems with asynchronous transmissions," *In Proceedings of the 54th IEEE Conference on Decision and Control, Osaka, Japan*, pp. 5494–5499, 2015.

[18] J. M. G. da Silva Jr., W. F. Lages, and D. Sbarbaro, "Event-triggered PI control design," *In Proceedings of the 19th IFAC World Congress, Cape Town, South Africa*, pp. 6947–6952, 2014.

[19] A. K. Behera, B. Bandyopadhyay, M. Cucuzzella, A. Ferrara, and X. Yu, "A survey on event-triggered sliding mode control," *IEEE Journal of Emerging and Selected Topics in Industrial Electronics*, vol. 2, no. 3, pp. 206–217, 2021.

[20] P. Dahiya, P. Mukhija, and A. R. Saxena, "Design of sampled data and event-triggered load frequency controller for isolated hybrid power system," *International Journal of Electrical Power & Energy Systems*, vol. 100, pp. 331–349, 2018.

[21] Z. Huo, "Distributed event-triggered robust automatic generation control for networked power system with wind turbines," *IET Renewable Power Generation*, vol. 15, pp. 562–573, 2021.

[22] X.-C. Shangguan, Y. He, C.-K. Zhang, L. Jin, W. Yao, L. Jiang, and M. Wu, "Control performance standards-oriented event-triggered load frequency control for power systems under limited communication bandwidth," *IEEE Transactions on Control Systems Technology*, vol. 30, no. 2, pp. 860–868, 2022.

[23] R. Goebel, R. Sanfelice, and A. Teel, *Hybrid Dynamical Systems: Modeling, Stability, and Robustness*. Princeton University Press, 2012.

[24] M. Fazeli, G. Asher, C. Klumpner, and L. Yao, "Novel integration of dfig-based wind generators within microgrids," *IEEE Transactions on Energy Conversion*, vol. 26, no. 9, pp. 840–850, 2011.

[25] M. Abdelrahim, R. Postoyan, and J. Daafouz, "Event-triggered control of nonlinear singularly perturbed systems based only on the slow dynamics," *In Proceedings of the IFAC Symposium on Nonlinear Control systems, Toulouse, France*, pp. 347–352, 2013.

[26] M. Abdelrahim, V. Dolk, and W. Heemels, "Input-to-state stabilizing event-triggered control for linear systems with output quantization," *In Proceedings of the 55th IEEE Conference on Decision and Control, Las Vegas, U.S.A.*, pp. 483–488, 2016.

[27] V. Dolk, D. Borgers, and W. Heemels, "Dynamic event-triggered control: Tradeoffs between transmission intervals and performance," *In Proceedings of the IEEE Conference on Decision and Control, Los Angeles, U.S.A.*, pp. 2764–2769, 2014.

[28] D. Carnevale, A. Teel, and D. Nešić, "A Lyapunov proof of an improved maximum allowable transfer interval for networked control systems," *IEEE Transactions on Automatic Control*, vol. 52, no. 5, pp. 892–897, 2007.

[29] D. Nešić, A. Teel, and D. Carnevale, "Explicit computation of the sampling period in emulation of controllers for nonlinear sampled-data systems," *IEEE Transactions on Automatic Control*, vol. 54, no. 3, pp. 619–624, 2009.

[30] M. Abdelrahim, R. Postoyan, J. Daafouz, and D. Nešić, "Robust event-triggered output feedback controllers for nonlinear systems," *Automatica*, vol. 75, pp. 96–108, 2017.